American Journal of Botany
Celebrating 100 years 1914–2014

American Journal of Botany 101(5): 875–885. 2014.

Flower morphology and floral sequence in *Artemisia annua* (Asteraceae)[1]

Hazel Y. Wetzstein[2,5], Justin A. Porter[2], Jules Janick[3], and Jorge F. S. Ferreira[4]

[2]University of Georgia, Department of Horticulture, 1111 Miller Plant Science Building, Athens, Georgia 30602-7273 USA; [3]Purdue University, Department of Horticulture and Landscape Architecture, 1165 Horticulture Building, West Lafayette, Indiana 47907-1165 USA; and [4]US Salinity Laboratory (USDA-ARS), 450 W. Big Springs Rd., Riverside, California 92507-4617 USA

- *Premise of the study: Artemisia annua* produces phytochemicals possessing antimalarial, antitumor, anti-inflammatory, and anthelmintic activities. The main active ingredient, artemisinin, is extremely effective against malaria. Breeding to develop cultivars producing high levels of artemisinin can help meet worldwide demand for artemisinin and its derivatives. However, fundamental reproductive processes, such as the sequence of flowering and fertility, are not well understood and impair breeding and seed propagation programs.
- *Methods:* Capitulum structure and floral sequence were studied using light and scanning electron microscopy to describe inflorescence architecture, floret opening, and seed set.
- *Key results:* Florets are minute and born in capitula containing pistillate ray florets and hermaphroditic disk florets. Ray florets have elongated stigmatic arms that extend prior to disk floret opening. Disk florets exhibit protandry. During the staminate phase, pollen is released within a staminate tube and actively presented with projections at the tip of stigmas as the pistil elongates. During the pistillate phase, stigmatic arms bifurcate and reflex. Stigmas are of the dry type and stain positively for polysaccharides, lipids, and an intact cuticle. Floret numbers vary with genotype, and capitula are predominantly composed of disk florets. Both ray and disk florets produce filled seed.
- *Conclusions:* Gynomonoecy, early opening of ray florets, and dichogamy of disk florets promote outcrossing in *A. annua*. For breeding and seed development, flowering in genotypes can be synchronized under short days according to the floral developmental stages defined. Floret number and percentage seed fill vary with genotype and may be a beneficial selection criterion.

Key words: artemisinin; *Artemisia annua*; Asteraceae; floral sequence; huang hua hao; pollen presentation; qinghao; Sweet Annie; wormwood.

Artemisia annua, (sweet Annie, annual wormwood, qinghao, huang hua hao), has been known for centuries as a medicinal plant. Native to China, the plant has become naturalized in regions including the United States, Europe, and South America. It has become a critical medicinal plant in recent times because it produces artemisinin, a potent compound against multidrug-resistant malaria. Recent studies show that *A. annua* produces bioactive metabolites possessing a number of pharmacological properties including potent anticancer activity (Crespo-Ortiz and Wei, 2012). As a widely used antimalarial compound, an important feature is that artemisinin has shown no significant side effects. Furthermore, *Artemisia* compounds exhibit anti-inflammatory, antibacterial, antiviral, and antiparasitic activities (Bhakuni et al., 2001).

Plant material is currently the economical source of artemisinin, with demand supplied through crop production. Artemisinin is commercially extracted from the leaves of cultivated and wild-grown plants, which produce and sequester artemisinin in glandular trichomes. Due to the low and variable content of artemisinin in *A. annua*, the demand for artemisinin cannot be met from current plant yields (Alejos-Gonzalez et al., 2011). Demand for a stable supply has resulted in complementary approaches, which include crop improvement and microbially based semi-synthesis to increase global artemisinin production (Immethun et al., 2013; Larson et al., 2013). Breeding to develop plants that produce high levels of pharmacologically active compounds has been an approach with recent efforts including the use of molecular techniques for development of a genetic map for *A. annua* (Graham et al., 2010).

The development of methods to produce large quantities of seed with high viability and vigor is critical for providing a reliable source of plant material. However, in order for successful hybridization to occur, flowering must be synchronized so that pollen release and stigma receptivity of parental lines coincide. As new improved cultivars become available, information on reproductive biology and seed production becomes vital. Thus, understanding the reproductive biology of *A. annua* is an important issue.

Some limited aspects of the floral morphology of *A. annua* have been described by Bailey (1951), Ohwi (1965), and Ferreira and Janick (1995). The general botany, horticulture, and pharmacology were reviewed by Ferreira et al. (1997). However, despite the importance of *A. annua* as a medicinal crop, fundamental features of reproductive biology including details of flower morphology, the sequence of flower opening, pollination biology, and seed development are poorly understood. An understanding of floral biology would provide valuable information for breeding and seed production programs. Thus, several key areas of investigation evaluating the reproductive biology of *A. annua* are proposed. The objectives of the present investigation were to study the morphology and histology of flowering in *A. annua* to (1) define inflorescence architecture and the floral sequence of ray and disk floret types, (2) evaluate stigma receptivity and pollen–stigma interactions, (3) assess flower fertility and seed set, and (4) characterize floral developmental

[1]Manuscript received 13 September 2013; revision accepted 17 April 2014.

[5]Author for correspondence (e-mail: hywetz@uga.edu)

doi:10.3732/ajb.1300329

stages needed to promote successful cross pollination. Our approach was to induce plants to flower under short-day treatments and to evaluate floral development over time using light and scanning electron microscopy. Further, plants grown in field plots were evaluated for floret numbers, fertility, and timing of floral developmental stages.

MATERIALS AND METHODS

Plant material—*Artemisia annua* L. is an annual herb that flowers under short days. Stock plants were obtained from seed derived from open pollination of lines from Brazilian (B) and Chinese (C) germplasm, and intercrosses of high-yielding lines (A), which were sown in flats containing Fafard 3B, a commercial potting mix containing peat moss, bark, perlite, vermiculite, and dolomitic limestone (Sun Gro Horticulture, Agawam, Massachusetts, USA). Plants were potted and maintained in the greenhouse under natural light conditions in the spring and summer. Because plants can attain heights of over 2 m, genotypes were maintained by periodically taking cuttings to control size and to increase the number of clonal plants for studies. During fall and winter, plants were maintained under long days (16 h light/8 h dark) to prevent flowering.

Flower timing, floret number, and seed set were evaluated using field-grown material of genotypes that were propagated from cuttings. Plants flowered under natural short day conditions during fall. The date of visible bud appearance was noted, and the timing to obtain the green bud stage (discrete green capitula enclosed within involucral bracts), yellow capitulum stage (bracts open exposing yellow floret buds), ray floret opening stage (pistillate ray flowers displaying stigmatic arms), and disk floret opening stage (hermaphroditic disk florets in the staminate stage undergoing pollen presentation and release) was determined. During full bloom, the number of total florets, pistillate ray florets, and hermaphroditic disk florets per capitulum were assessed by dissecting under a microscope ($n = 50$ capitula per genotype). At seed maturity, capitula were collected ($n = 50$ per genotype), dissected apart, and the number of filled and aborted seed from ray and disk florets determined.

For floral morphology and flower sequence studies, potted plants in 19 cm diameter, 3.8 L pots were induced to flower by placing them in growth chambers under a photoperiod of 9 h light/15 h dark, at 22°C day/18°C night. As capitula formed, samples were collected and observed over time. For evaluations of pollen–stigma interactions, individual plants were isolated to prevent cross pollination. Small clusters of inflorescences were removed from plants and the stems placed in water. Capitula were examined under a dissecting microscope to ensure the stigmas were free of pollen. Using pollen from just-opened disk florets, we hand-pollinated ray and disk florets with expanded stigmas by dusting with pollen that was loaded onto a fine artist paint brush held over the stigmatic surface. Pollen from plants of Chinese germplasm was used to pollinate plants of Brazilian germplasm, and visa versa.

Pollen to ovule ratios were determined by dividing the number of pollen grains per floret by the number of ovules per floret. Single disk florets were teased apart on a slide containing lactophenol with 0.1% (w/v) aniline blue to release pollen grains. The whole mounts were digitally photographed at 40× magnification to include all pollen grains, and pollen grains per floret were counted. Ten disk florets for each of the six genotypes were used, collected from three to four capitula from a single cloned plant for each genotype.

Scanning electron microscopy (SEM)—Florets were dissected and prepared using methods described by Wetzstein et al. (2011) for SEM. Florets were fixed in 2% (v/v) glutaraldehyde in 0.1 mol/L cacodylate buffer, pH 7.2, dehydrated in an ethanol series, and critical-point-dried through carbon dioxide using a critical point drier (Samdri-790; Tousimis Research, Rockville, Maryland, USA). Dried samples were mounted on aluminum stubs using carbon conductive tabs and sputter coated (SPI-Module; SPI Supplies, West Chester, Pennsylvania, USA) with gold. In addition, SEM observations of fresh, unfixed samples were conducted to provide information on pollen–stigma interactions and stigmatic exudate development. Samples were examined using a SEM (JSM 5800; JEOL, Tokyo, Japan) at 15 kV.

Light microscopy (LM)—Inflorescences were collected and dissected, and tissues were fixed overnight in ethanol–acetic acid (3 : 1, v/v). For clearing, samples were transferred into 10% sodium sulfite (w/v), and then autoclaved at 120°C for 10 min. Individual florets were mounted on microscope slides as cleared samples or following additional staining. For general viewing, tissues were stained in 1% aqueous acid fuchsin (w/v), followed by 0.5% aqueous toluidine blue (Feder and O'Brien, 1968). Carbohydrates were visualized with periodic acid–Schiff's (PAS) reagent (Pearce, 1972). For lipid detection, florets were stained in 0.3% Sudan black B (w/v) in 70% ethanol, and destained in 70% ethanol. Cuticle was visualized by staining in 0.01% auramine O in 0.05 mol/L phosphate buffer, pH 7.2 (Heslop-Harrison, 1977) and viewed under blue fluorescence (excitation BP460-490, barrier BA520) using an X-Cite 120 Fluorescence Illumination System (Excelitas Technologies, Mississauga, Ontario, Canada). Tissues were examined using a light microscope (BX51; Olympus America, Center Valley, Pennsylvania, USA) and photographed digitally.

RESULTS

Floral organization—Florets are minute (<2 mm long) and borne within small disk-shaped capitula (2–3 mm wide) which are organized in loose spreading panicles (Fig. 1A). Characteristic of the Asteraceae, each capitulum contains two floret types: (1) marginal ray florets, which are pistillate, and (2) central disk florets, which are hermaphroditic (Fig. 1B). Florets are sessile and the inferior ovary is attached to a mound-shaped receptacle (Fig. 1C). Numerous glandular trichomes, the site of artemisinin production, are present on floral surfaces including the receptacle and corolla of florets. Numerous developing inflorescence buds were evident at 24 d after the onset of short day treatments (Fig. 1D). Inflorescences are subtended by an elongated bract (Fig. 1A, D) and further enveloped by numerous imbricate involucral bracts. At maturity, capitula are nodding and display the numerous yellow florets that make up each inflorescence, as shown in Fig. 1E. The number and type of florets per capitulum varies. Table 1 summarizes the total number of florets, the mean number of ray florets, and ray to disk floret ratios per capitulum for six different *A. annua* genotypes. Significant differences in the total number of florets per capitulum were observed among genotypes with values ranging from 20 to 29 florets. The genotype producing the highest number of florets, B4, produced 1.4 times more florets than the lowest producing genotype, B6. Ray floret numbers per capitulum were lower than disk florets numbers in all genotypes. Ray to disk floret ratios ranged from 0.34 to 0.61. Using the G test for heterogeneity, there was no evidence that the ray to disk floret ratio varied among genotypes ($G = 1.17$, df = 5, $P = 0.95$).

Flower opening sequence—Opening capitula with visible florets are evident 36 d after the initiation of short day treatments (Fig. 2A). The staggered development of florets within an inflorescence is evident, with the opening of the marginal ray florets preceding that of the central disk florets. Corresponding LM and SEM images of similar-stage capitula are shown in Fig. 2B and C. Early emergence of the bifurcated stigmas of ray florets is evident before the opening of disk florets; central disk florets at this time are for the most part closed, with no to few central buds beginning to open. The dual stigmas of ray florets emerge from apical openings formed from the separation of 2–3 ligulate lobes (Fig. 2D). Cleared samples show how stigmas emerge from a tubular corolla, which at this stage encloses an elongate style (Fig. 2E). The ovary is inferior and unilocular. Glandular trichomes are found on the leaves, bracts, and corolla (Fig. 2E insert, Fig. 2C, D), but are lacking on stigma, style, and ovary (Fig. 2E, F). Further elongation of the stigma and style follows, resulting in expansive stigmatic arms bifurcating from a style that now extends beyond the corolla's tubular sheath (Fig. 2F). The elongated stigmatic arms are lined with papillae, which are restricted to two ventro-marginal bands (Fig. 2G, H).

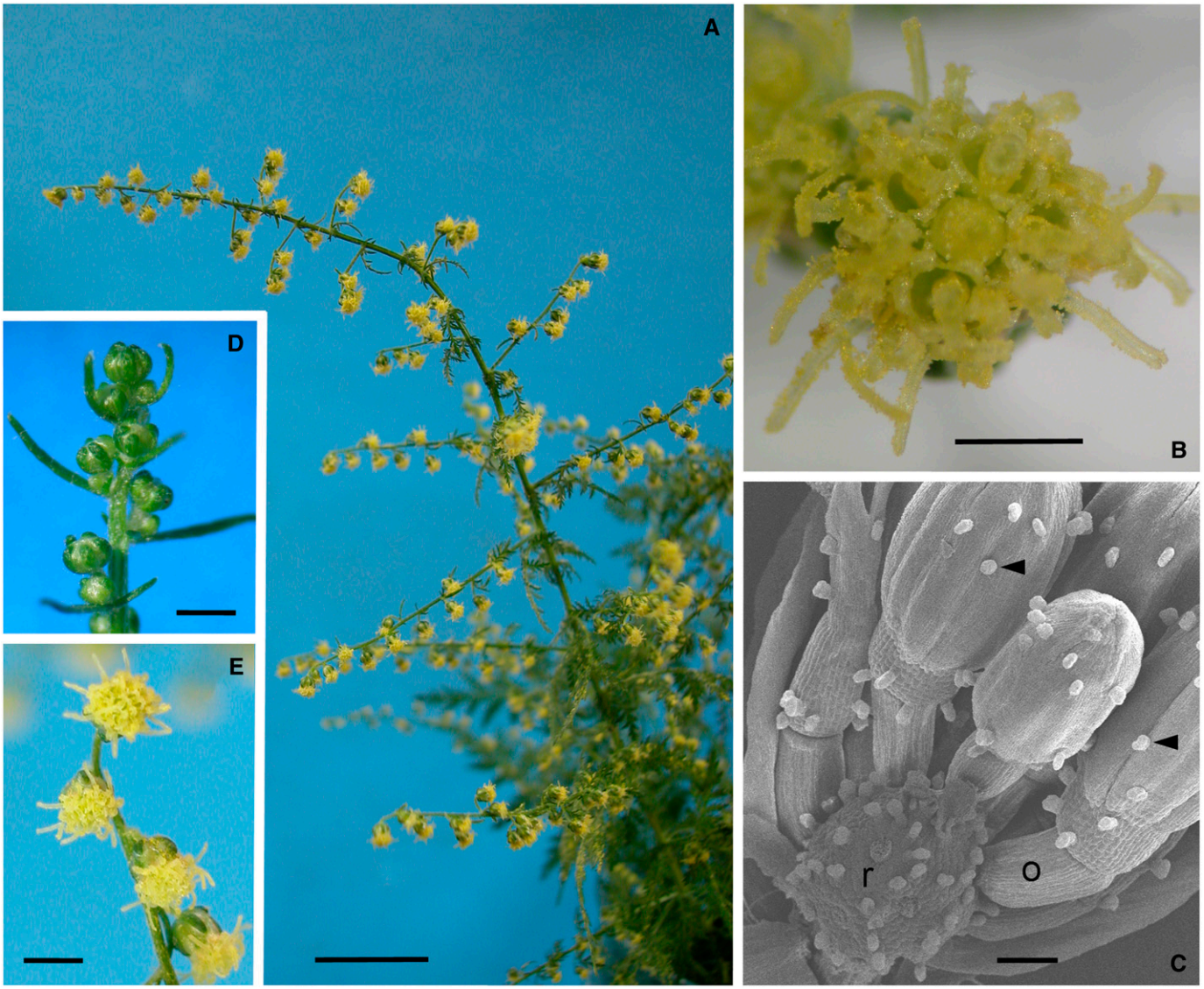

Fig. 1. Inflorescences of *Artemisia annua*. (A) Capitula are numerous and organized in loose, spreading panicles. (B) A capitulum showing marginal ray florets and central disk florets. (C) SEM of a dissected young inflorescence showing sessile florets with an inferior ovary (o) attached to a mound-shaped receptacle (r). Florets have not yet opened. Glandular trichomes (arrowheads) are visible. (D) Inflorescence buds at 24 d after the onset of short-day treatments. (E) Capitula with numerous open florets 45 d after short-day treatment. Bars = 2 cm (A), 1 mm (B), 200 μm (C), 3 mm (D, E).

Stigmatic surface cells are unicellular and papillose, with a prominent, central protuberance (Fig. 2I).

The corolla of disk florets is covered with numerous glandular trichomes (Fig. 3A). Dissections removing the corolla expose a tubular cage-like structure formed from the fusion of the five stamens (Fig. 3B). This androecial tube terminates in five acuminate apical extensions. Disk florets are sympetalous and have a campanulate corolla upon opening, separated at the apex into five distinct pointed lobes (Fig. 3C). A top view of florets (Fig. 3D) at the closed bud stage shows the apical region where separation of the corolla will occur; an early-opening floret with a reflexed corolla exposes the top of the anther tube with its antepetalous crown-like structure. At later stages when disk florets open, capitula change orientation from upright (Fig. 1D) to nodding (Fig. 1E). A floret split longitudinally and partially flattened shows linear arrays of fused dithecous anthers that form a tube around the style (Fig. 3E). Anthers dehisce inward, along their entire length, which facilitates pollen release toward the floral axis and pollen accumulating at the floral apex due to gravity. At this time, the stigma is short, immature and linear, but divided into two stigmatic lobes held upright and tightly appressed. Disk florets exhibit protandry and release pollen with an active pollen presenter prior to stigma receptivity. During the staminate phase, as the pistil elongates, modified plumose projections at the tip of the upright stigma facilitate the movement of pollen grains from the interior of the anther tube toward the opening of the pendant floret, thereby presenting pollen from the anthers for dissemination (Fig. 3F). Subterminal projections composed of marginal papillae are visible in lateral view along the edge of the juxtaposed stigmatic arms. Pollen adherence on immature stigmas was not observed. Accumulation of pollen often occurs at the crown region of the

TABLE 1. Number of total florets and ray florets and ray to disk floret ratios per capitulum, and pollen to ovule (P/O) ratios for six genotypes of *Artemisia annua*.

Genotype	Total floret no.	Ray floret no.	Ray to disk ratio	P/O ratio
B4	28.8 ± 0.67 a	7.0 ± 0.11	0.34 ± 0.01	2071 ± 21
C1	26.0 ± 0.54 b	6.7 ± 0.14	0.37 ± 0.17	2243 ± 65
B10	23.1 ± 0.64 c	8.0 ± 0.16	0.61 ± 0.04	2867 ± 104
C10	21.3 ± 0.47 cd	7.0 ± 0.11	0.52 ± 0.02	2393 ± 60
A63	20.5 ± 0.58 d	6.1 ± 0.16	0.45 ± 0.02	1897 ± 43
B6	20.3 ± 0.54 d	6.9 ± 0.22	0.56 ± 0.03	2516 ± 32

Notes: For floret counts, $n = 50$ capitula per genotype. For counts for pollen to ovule ratios, $n = 10$ disk florets per genotype; values are means ± SE. Means within the same column followed by the same letter are not significantly different according to Tukey's test at $P \leq 0.05$.

anther tube (which projects toward the open corolla), resulting in the formation of a pollen plug (Fig. 3G). Pollen is discharged and presented (Fig. 3G, H) with elongation of the pistil and extrusion of the stigma. The cleared floret in Fig. 3H shows the ovary, outline of the corolla, and internally the central style and nonprotruding stamens (darker regions within the cleared corolla), which have released their pollen. Pollen is yellow at dehiscence, separate and nonclumping, tricolpate, and smooth with microechinate ornamentation (Fig. 3I). Pollen to ovule ratios for disk florets of different genotypes range from about 1900 to 2800 (Table 1); florets contain a single ovule.

Disk florets in more advanced capitula have open florets with exposed stigmas at varying stages of emergence and bifurcation (Figs. 4A vs. 2C). Ray florets, which opened earlier, have fully extended stigmatic arms. During early stigma emergence of disk florets, the terminal presenter portion of the stigma containing elongated epidermal hairs is visible pushing through the crown-like opening of the staminal tips (Fig. 4B). Pollen that accumulated as a plug is pushed out, as evidenced by residual pollen grains at the apical portion of the stigma, adhering to the pollen presenter region. The pistillate stage of disk floret development follows. As the stigma and style further elongate and extend beyond the corolla, the stigmatic arms bifurcate and begin to reflex, exposing an extensive papilloid stigmatic surface (Fig. 4C). Residual self-pollen is in some cases retained on the tips of the elongated hairs of the presenter (Fig. 4D). At maturity, stigma lobes are fully expanded and contain stigmatic papillae positioned along two marginal rows (Fig. 4E) similar to that found in ray florets (Fig. 2G). Stigmatic papillae appear identical in the two floret types (Fig. 4F, 2I), both being unicellular with a central projection. Stigmas lack copious exudate, as characteristic of dry stigma types. Histochemical staining of both floret types with periodic acid–Schiff's reagent was strongly positive for polysaccharides on the stigma arms, faint for the style region near the stigma, and absent for the ovary and corolla (Fig. 4G). Likewise, lipids were visualized only on stigmas in both disk (Fig. 4H) and ray (Fig. 4I) florets. As expected with dry stigma types, an intact cuticle was observed when stigmas were stained with auramine O, as shown in companion micrographs of the reflexed stigma of a disk floret viewed under transmitted (Fig. 4J) and fluorescent (Fig. 4K) illumination. Pollen that adhered to the reflexed pollen presenter region exhibited strong auto fluorescence.

Pollen capture occurs over the length of the exposed stigma on papillate cells (Fig. 5A), facilitated by the size and spacing of the projections on the stigmatic surface, often nesting among nipple-like protrusions (Fig. 5B, C). At 6 h after pollination, swelling protuberances at germination pores can be observed (Fig. 5C). The stigmatic region located between the two rows of stigmatic papillae is composed of smooth rectangular-shaped cells that are devoid of pollen and do not participate in pollen capture (Fig. 5C). Also at 6 h, pollen grains have started to germinate and pollen tubes to emerge (Fig. 5D). At 16 h, pollen tubes are elongating and penetrating the stigma (Fig. 5E, F). Secretion of stigmatic exudate following pollination was not observed with SEM. Persistent brown stigmas (Fig. 5G) with adhering residual pollen (Fig. 5H) are evident on florets of older capitula at 20 d post pollination. Corolla tubes in both disk and ray florets remain green at the base above enlarged, light-green ovaries (Fig. 5I, J). The fertility of ray and disk florets and their ability to set viable seed are shown in Table 2. Florets exhibited from 40 to 51% filled seed, with ray florets producing higher percentages of filled seed than disk florets. However, disk floret number per capitulum was over 2.5 times that of ray florets; thus seed production was predominantly from disk florets due to the higher numbers of flowers of this type.

Floral development in *A. annua* follow a series of developmental stages depicted in Fig. 6. Vegetative shoots (Fig. 6A) under inductive short day conditions initiate numerous, small inflorescence buds (Fig. 6B; similar to 1D). As shoots develop, these inflorescences enlarge with each green capitulum enclosed within involucral bracts (Fig. 6C). As bracts separate, floret buds become exposed, and the capitula take on a yellow-green color (Fig. 6D). With further expansion of florets, ray florets open and display elongate stigmatic arms (Fig. 6E; similar to Figs. 2B, C). The capitula at this stage are yellow. In a later stage (Fig. 6F), capitula are larger, yellow, and have open hermaphroditic florets that are in the staminate stage when pollen presentation and release is occurring (similar to Fig. 3G). Disk florets with pollen plugs or which have discharged their pollen are evident. Ray florets have fully extended stigmatic arms. In the last stage shown (Fig. 6G), disk florets are in the pistillate stage with exposed and reflexed stigmatic arms (as in Figs. 1A, 1E, 4A). Pollen release has already occurred. The timing of this floral sequence under field conditions is shown in Table 3. Days from the first appearance of inflorescence buds (Fig. 6B) until specific stages of ontogeny (Fig. 6C–G) are shown. The days from visible bud to open disk florets ranged from 19 d (B4 genotype) to 24 d (B6 genotype). For the six genotypes evaluated, opening of ray florets occurred within 3 d of each other. The delay in opening of disk flowers ranged from 3 d in genotype C1 to 7 d in genotypes B4, A63, and C10.

DISCUSSION

Although the Asteraceae contain agriculturally and horticulturally important species, there are few detailed studies on flowering or pollen–stigma interactions in this family (Hiscock et al., 2002). A clear understanding of floral morphology and function is of significant importance to breeding programs and for production of high quality seed. Thus, floral architecture, developmental timing of ray and disk florets, pollen–stigma responses, and flower fertility/seed-set evaluations in *A. annua* were depicted in the present study.

***Flower structure and inflorescence development*—**Flowering in *A. annua* is readily induced when apical meristems perceive short day conditions. Inflorescence buds are visible in

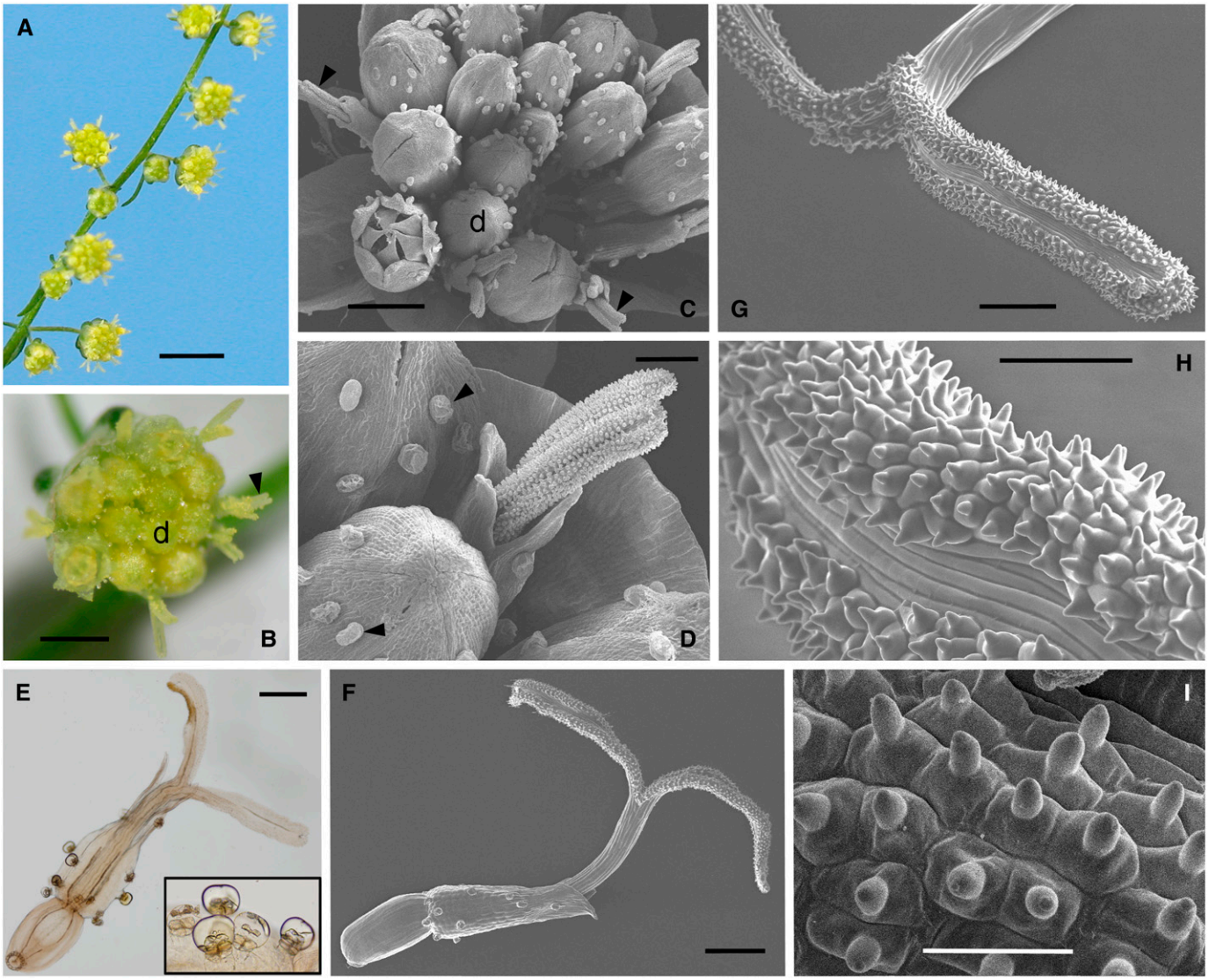

Fig. 2. Inflorescences and florets of *Artemisia annua*. (A) Capitula at 36 d after the initiation of short days. Some florets are beginning to open. (B) Close up of a capitulum at the stage of early floret opening. Ray floret opening and emergence of stigmas (arrowhead) generally precedes that of the central disk (d) florets, which are mostly still closed buds. (C) Corresponding SEM image of a capitulum similar to that shown in image B. Early emergence of the stigmatic arms (arrowhead) of pistillate ray florets is evident. Hermaphroditic disk florets (d) are closed, except for one floret bud that has started to open. (D) SEM showing the two stigmatic arms of a ray floret emerging from the apical opening of the corolla. Glandular trichomes (arrowhead) are evident on closed disk florets. (E) Cleared ray floret, and close up of glandular trichomes (insert). (F) SEM of a more developed ray floret with elongated style and extended stigmatic arms. (G) SEM of stigmatic arms of a ray floret showing stigmatic papillae along two ventro-marginal bands. (H) SEM close up of stigmatic surface of a ray floret. (I) SEM of stigmatic surface showing unicellular cells with prominent central protuberances. Bars = 1 cm (A), 1 mm (B, C), 200 μm (D, G), 400 μm (E, F), 50 μm (H), 25 μm (I).

some genotypes within 2.5 wk of short day treatment. However, the number of days to flowering and anthesis following the onset of short day treatments can be variable and appears to be specific to genotype. For example, at 36 d, genotypes range from those having capitula with open ray and disk florets, to those with capitula that are tightly enclosed within involucral bracts. Thus, in breeding programs, knowledge of the timing of flower development in key genotypes, as well as the relative developmental timing of ray and disk florets is of critical importance for successful crossing.

Artemisia annua produces small, nodding capitula (2–3 mm in diameter), composed of pistillate ray florets that incompletely line the periphery of the inflorescence and centrally located hermaphroditic disk florets. The average number of florets per capitulum is 20 or more and significantly varies with genotype; a 1.4-fold difference occured in the material evaluated in the present study. The receptacle resembles a flattened cone and harbors glandular trichomes, as do the florets. Floret types within a capitulum differ in the timing of opening and maturation. Pistillate ray floret opening and stigma extension precede that of the hermaphroditic disk florets. Further, the two flower types have divergent pistil organization, i.e., ray floret stigmas have long filiform stigmatic arms in contrast to the broad recurving stigmas observed in disk florets with elongated terminal

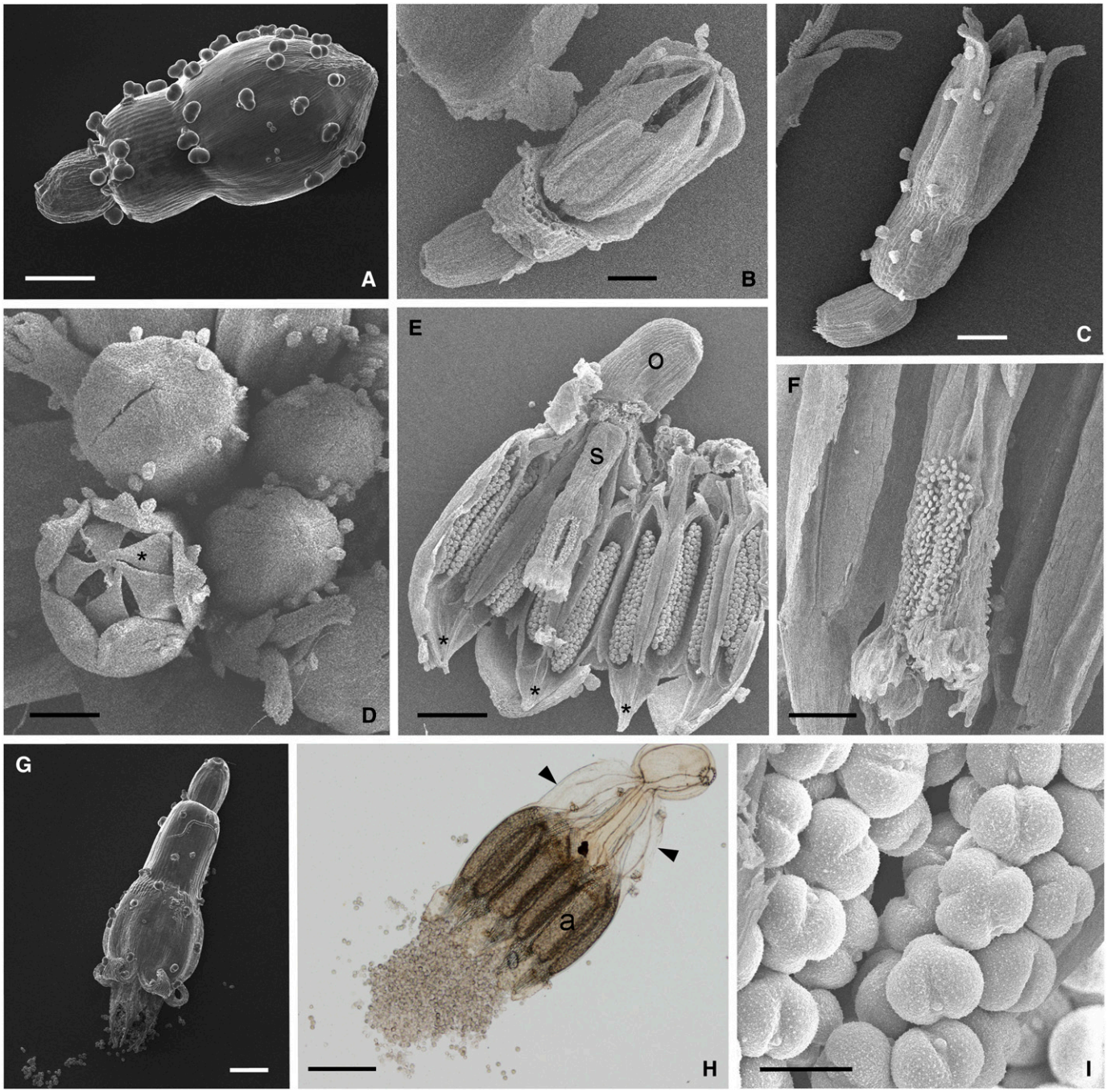

Fig. 3. Disk florets in *Artemisia annua* at the closed bud and staminate phases. (A) SEM of closed bud of a disk floret with numerous glandular trichomes on the corolla. (B) SEM of floret as in (A) with corolla removed, exposing an androecial tube with acuminate apical extensions. (C) SEM of partially open disk floret showing campanulate corolla and distinct apical lobes. (D) SEM of top view of florets in a capitulum. An early opening floret with reflexed corolla exposes the top of the anther tube, which forms a crown-like structure (marked with asterisk). (E) SEM of a floret split longitudinally and partially flattened showing ovary (o), central style (s), and linear arrays of fused dithecous anthers that form a staminal tube that surrounds the style. Asterisks denote apical extensions of the androecial tube. (F) SEM close up of the apical portion of an immature stigma. Plumose projections at the tip of the upright stigma act as a secondary pollen presenter. (G) SEM of bisexual floret discharging pollen. (H) Cleared LM of bisexual floret showing the ovary, outline of the corolla (arrowheads), introrsely dehiscing anthers (a), and released pollen. (I) SEM of tricolpate, microechinate pollen. Bars = 500 μm (A–E, G, H), 200 μm (F), 50 μm (I).

hairs; apical regions of ray floret stigmatic arms lack modified papillae. In other Asteraceae species, the styles of ray florets likewise have been reported to be more slender and have no or less-developed papillate sweeping hairs than hermaphroditic florets (Torres and Galetto, 2007).

Glandular trichomes are abundantly found on both ray and disk floret types. The biosynthesis and sequestration of artemisinin is within these glandular secretory trichomes (Duke and Paul, 1993; Tellez et al., 1999; Olsson et al., 2009). The glandular trichomes observed in floral parts or *A. annua* are

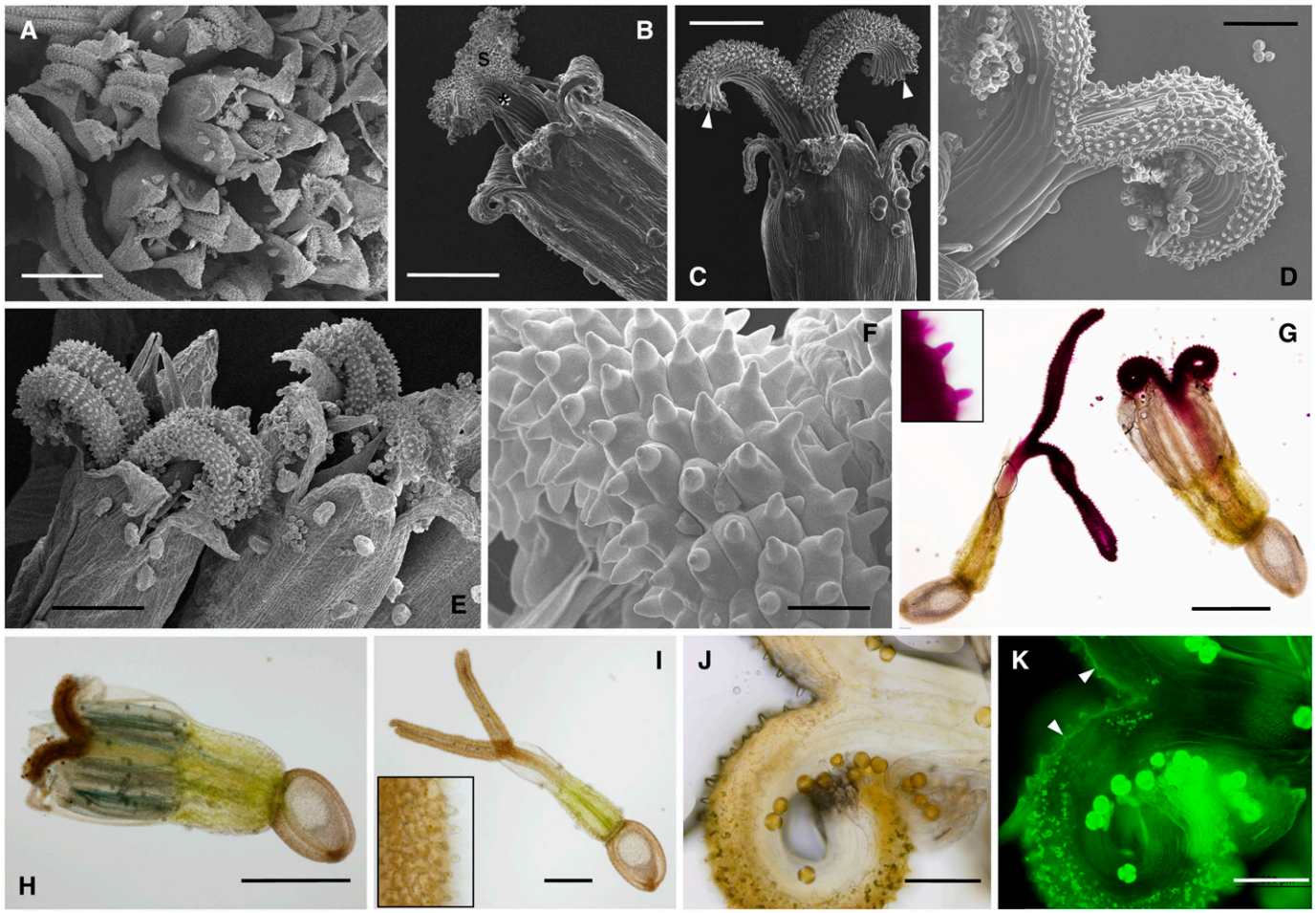

Fig. 4. Florets in *Artemisia annua*. (A) SEM of a more advanced capitulum (vs. Fig. 2C) with disk florets at different stages of stigma emergence and bifurcation and a ray floret (at left) with elongated, filiform stigmatic arms. (B) SEM of disk floret with stigma (s) emerging beyond anther tips (*). (C) SEM of disk floret with elongated stigma and style; stigmatic arms are bifurcate and reflexed. The terminal pollen presenter (arrowhead) portion of the stigma is visible. (D) SEM of fully reflexed stigmatic arms with residual pollen retained on the tips of elongated presenter papillae. (E) SEM of disk florets with expanded stigma lobes showing stigmatic papillae along two marginal rows. (F) SEM close up of stigmatic papillae. (G) LM whole mount of pistillate ray (left) and hermaphroditic disk (right) florets stained with periodic acid–Schiff's reagent showing positive staining for polysaccharides on the stigma. (H) LM of disk floret showing positive Sudan black B lipid staining on stigmas. (I) LM of ray floret showing positive Sudan black B lipid staining on stigmas. Close up of stigmatic papillae of ray floret (insert). (J, K) Corresponding areas of the stigma from a disk floret stained with auramine O viewed with (J) transmitted and (K) fluorescent illumination. An intact cuticle (arrowheads) is evident in (K). Bars = 1 mm (A, G, H), 500 μm (B, C, E), 200 μm (D, I-K), 50 μm (F).

similar to those described on the leaves. Glandular hairs are 10-celled biseriate structures composed of two stalk cells, two basal cells, and three pairs of secretory cells (Duke and Paul, 1993; Ferreira and Janick, 1995). Although present on the bracts, receptacle, and corollas of florets, glandular trichomes were conspicuously absent from the pistil. The artemisinin content varies in different plant organs and with plant developmental stage and environmental conditions (Zhang et al., 2006; Arsenault et al., 2010; Kjaer et al., 2013). Different densities of capitate trichomes on the surface of leaves, flowers, and branches have explained variations in artemisinin content of plant parts (Zhang et al., 2006).

On the basis of the SEM evaluations of both fresh and fixed tissue, the stigmatic surface of *A. annua* lacks a copious exudate and can be classified as having a dry stigma type. Histochemical staining indicates that the stigmas of both ray and disk florets contain lipids, polysaccharides, and a surface cuticle. Polysaccharides and lipids are confined primarily to the region of the stigmatic arms; staining is absent in the ovary, style, and corolla. Pollen adherence, pollen hydration, and germination are not associated with a promotion of exudate production. Based on evaluations of 17 species, the stigmas of members of the Asteraceae have been described as dry (Heslop-Harrison and Shivanna, 1977). However, some Asteraceae have been observed to produce small amounts of extracellular secretions between stigmatic papilla cells, which has led to the suggestion of a "semi-dry" classification for some members of this group (Hiscock et al., 2002).

The papillae on the stigmatic surface in *A. annua* are arranged into two ventro-marginal bands along each style branch as has been reported in some members of the same subfamily (Bremer, 1994; Torres and Galetto, 2007). The morphology of stigmatic cells in ray and disk floret types is indistinguishable; both floret types have unicellular surface cells with a centrally

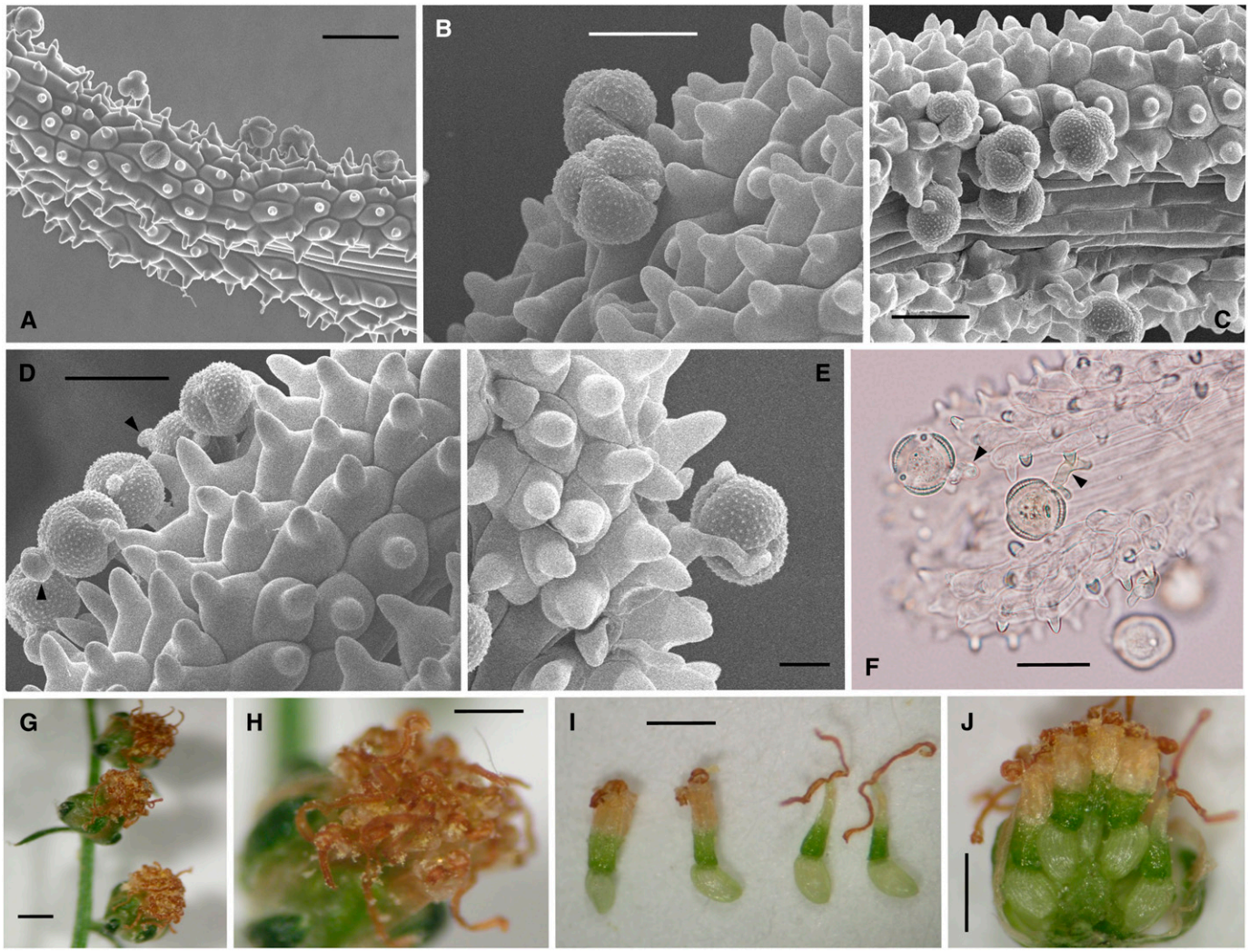

Fig. 5. Pollinated florets in *Artemisia annua*. (A) SEM of pollinated stigma from a ray floret. (B) SEM showing that pollen capture is facilitated by the spacing of the projections on stigmatic surface papillae; pollen often nests among nipple-like protrusions. (C) SEM of pollen adhering to papillate regions on stigmatic lobes, which are located along two ventro-marginal rows. (D) SEM at 6 h after pollination: germination pores have swelling protuberances and emerging pollen tubes (arrowhead). (E) SEM of an elongated pollen tube. (F) LM of pollen tube elongation (arrowhead) and penetration into the stigma 16 h after pollination. (G) Capitula 20 d after pollination. (H) Stigmas are desiccated and brown with residual pollen adhering. (I) Disk (left) and ray (right) florets from a capitulum as in (G). Stigmas are brown; ovary has expanded. (J) Dissection of a capitulum showing developing ovaries derived from pollinated florets. Bars = 100 μm (A), 50 μm (B–D, F), 25 μm (E), 2 mm (G), 1 mm (H–J).

raised projection that facilitate pollen capture between protrusions. This result concurs with a study comparing style morphological diversity of 42 species of the Asteraceae where stigmatic area organization and the morphology of stigmatic papillae are identical in all species that had dimorphic florets (Torres and Galetto, 2007).

***Breeding/pollination systems*—**Pollen presenters, i.e., floral structures other than anthers from which pollen is relocated and distributed, occur in all taxa in the Asteraceae, and may offer a selective advantage by providing greater accuracy in pollen transfer than with normal anther to stigma transfer (Ladd, 1994). Style morphology can be quite diverse within the Asteraceae where divergent morphology and organization of pollen presenter and pollen receptive structures has been described (Ladd, 1994; Torres and Galetto, 2007). Style types can vary in the arrangement of sweeping hairs and range from types with hairs scattered dorsally along the style branches at varying distances along the stylar shaft, to types with hairs grouped in a ring below the style bifurcation, or those with hairs confined to upper portions of the style branches. In *A. annua*, a pollen presenter forms in disk florets from sterile papillae confined to the tip region of upright stylar branches. At this time, capitula become pendant and released pollen often aggregates in a plug at the crown region of the anther tips. As the stigma further extends, pollen is pushed outward as the style elongates within the staminal tube and beyond the anther tips.

The palynological features of *A. annua* observed in the present study are typical for that described for related genera in the Asteraceae. A similar pollen type with three colpi and pores was described for *A. absinthium* (Konowalik and Kreitschitz, 2012) and *A. granatensis* (Penas et al., 2011). In a study comparing

TABLE 2. Number of filled seeds, abortive seeds, and percentage seed set per capitulum for ray and disk florets of *Artemisia annua*.

Floret type and characteristic	C1 genotype	A137 genotype
Ray florets		
No. of filled seeds	3.7 ± 0.20	3.4 ± 0.24
No. of abortive seeds	3.6 ± 0.20	4.0 ± 0.26
Seed set (%)	50.7 ± 2.5	46.5 ± 3.06
Disk florets		
No. of filled seeds	8.4 ± 0.37	7.9 ± 0.45
No. of abortive seeds	10.9 ± 0.40	12.2 ± 0.56
Seed set (%)	43.7 ± 1.8	39.5 ± 1.82
All flower types		
No. of total florets	26.6 ± 0.44	27.5 ± 0.72
Seed set (%)	45.7 ± 1.5	41.3 ± 1.52

Notes: Seed assessments were determined with $n = 50$ capitula per genotype. Values are ±SE.

Artemisia and related genera, pollen was similarly 3-zonocolporate, isopolar with radial symmetry, and microechinate (Martin et al., 2001). Pollen in *A. annua* is nonclumping, microechinate, and readily carried in wind currents following active pollen presentation in the pendant disk florets. Florets are minute, nonshowy, and lack nectaries. Two pollination modes have been suggested in the Anthemideae tribe of the Asteraceae: anemophily in *Artemisia* and its immediate allies, and entomophily in the remaining genera (Mucciarelli and Maffei, 2002). Our observations support that anemophily is the dominant mode of pollination in *A. annua.*

Although artemisinin biosynthesis in progeny of self-pollinated *A. annua* plants has been reported (Alejos-Gonzalez et al., 2011), studies suggest that the species favors cross-pollination with selfing rates of about only 1% (Delabays et al., 2001). A survey of the breeding systems of 571 species in the Asteraceae revealed that self-incompatibility occurs in the majority (68%) of plants; 10% of plants were partially self-incompatible and 27% of plants self-compatible (Ferrer and Good-Avila, 2007). Evolution of the breeding system has been dynamic in this family. Self-incompatibility has been suggested to occur in *A. annua*, primarily because self-pollinated plants, i.e., plants of a single genotype grown in isolation, are reported to produce few viable seeds. Critical evaluations describing pollen-stigma interactions following cross- and self-pollinations are lacking in *A. annua*. Cruden (1977) found evidence indicating that pollen to ovule ratios reflect plant breeding systems, where cleistogamous flowers have relatively low pollen to ovule ratios, selfing plants somewhat higher ratios, and outcrossing plants even higher ratios. The mean pollen to ovule ratio for the six *A. annua* genotypes was found here to be 2331 and is within the low range of wind-pollinated outcrossers. Other flowering characteristics found in this species that may promote outcrossing include protandry and gynomonoecy (Bertin and Newman, 1993; Pugnaire and Valladares, 2007). The dichogamy in disk florets is strongly protandrous with no overlap in male and female function. Pollen release in disk florets well precedes the emergence of stigmatic lobes. Gynomonoecy is further associated with differential timing in the opening of ray and disc florets. Outcrossing is promoted by early stigma expansion in pistillate ray florets that precedes disk floret opening and pollen release.

Data on the timing of flowering stages indicate that the stage when ray florets are open with receptive stigmas is 4 to 7 d before disk florets release pollen. Thus, the pollen available to ray florets is likely to be from another source, similar to disk florets, which have complete dichogamy. This flower development strongly promotes outcrossing in that pollen is mandatorily received from another floret. Uniformity of flowering within a plant readily allowed overall rating of flower stages. However, *A. annua* plants produce prolific numbers of capitula with some staggered flower development such that capitula on the same plant are not all synchronous. Thus, geitonogamy is possible with pollen transfer between early protandrous disc flowers and late pistillate ray flowers and/or pollen transfer from disc florets on a late capitulum in the staminate phase to disc

Fig. 6. Floral developmental stages in *Artemisia annua* showing from left to right, earlier and later stages, respectively. (A) Vegetative shoot. (B) Reproductive shoot with inflorescence buds similar to that shown in Fig. 1D. (C) The green bud stage with capitula that are discrete, green, and enclosed within involucral bracts. (D) The yellow capitulum stage with bracts of capitula that are open, exposing the yellow-green floret buds, which are closed. (E) Capitula showing expansion of florets; ray florets have opened and display stigmatic arms similar to that shown in Fig. 2B, C. (F) Disk florets are opened and in the staminate stage when pollen presentation and release are occurring. (G) More advanced capitula with disk florets in the pistillate stage with exposed and reflexed stigmatic arms, similar to that shown in Figs. 1E and 4A.

TABLE 3. Timing of flowering stages in relation to the occurrence of visible inflorescence buds for plants grown in field plots in Athens, Georgia.

		Days from visible buds			
Genotype	Visible buds (date)	Green bud stage	Yellow capitulum stage	Open ray florets	Open disk florets
A137	14-Sept	8	13	18	22
B6	15-Sept	10	16	19	24
C1	15-Sept	11	15	17	20
C10	16-Sept	11	14	16	23
A63	17-Sept	8	11	14	21
B4	19-Sept	4	9	12	19

Notes: Green bud stage, capitula are discrete, green, and enclosed within involucral bracts; yellow capitulum stage, bracts enclose capitula that are open, exposing yellow floret buds that are closed; open ray floret stage, pistillate ray florets are open and display stigmatic arms, and disk floret buds are closed; open disk floret stage, open hermaphroditic disk florets are in the staminate stage when pollen presentation and release are occurring.

florets on an earlier capitulum in the pistillate stage. Poor or no seed production has been reported in isolated plants.

Female fertility and seed set—Total floret number varied significantly with genotype. Seed set and yield may be important characteristics to include in selection programs. This study confirms the female fertility of both ray and disk florets in *A. annua* and their ability to set viable seed. Both ray and disk florets have well-developed stigmas, styles, and ovaries. Stigmatic cells in both floral types stained positively for carbohydrates and lipids and supported pollen hydration and germination. The percentage filled seed was over 40% for both ray and disk florets in all genotypes evaluated. Viable seed development from both ray and disk florets has also been observed in other members of the Asteraceae (Imbert et al., 1996; Gibson and Tomlinson, 2002). However, reports of flower fertility in other species in the Asteraceae are variable with differences among flower types observed and sterility noted in some flower morphs. In *Echinacea pallida*, the outer whorl of ligulate ray florets is sterile with florets lacking a full gynoecium (Wist and Davis, 2008). Similarly, the capitula of *Centaurea cyanus* have sterile ray florets and fertile disk florets. In some cases, seed heteromorphism occurs with variations in germination and dispersal between central vs. marginal achenes in a capitulum.

In practice, when controlled crossing is desired for breeding or seed production, selected parental genotypes are isolated during flowering, and the resultant seed collected are thought to be derived from cross- and not self-pollination. Flower induction and timing to produce plants appropriately staged (as shown in Fig. 6) to serve as pollen donors (disk florets at the staminate stage) or as receptive females (ray florets or pistillate-staged disk florets) are required.

Conclusion—Breeding to develop high-artemisinin-producing cultivars in conjunction with developing efficient protocols for seed production of improved genetic material is an approach to help meet worldwide demand of artemisinin and its derivatives. Flower structure and the sequence of floret opening were evaluated in *A. annua* using light and scanning electron microscopy to define the developmental stages of floret types within inflorescences and to evaluate stigma morphology and pollen–stigma interactions. Florets are minute and borne in capitula containing pistillate ray florets and centrally located hermaphroditic disk florets. Outcrossing is promoted by the differential timing of ray and disk floret opening within a capitulum (i.e., bifurcated stigmas of ray florets extend prior to the opening of disk florets), and by dichogamy of hermaphroditic disk florets. Pollen dissemination in disk florets is via secondary pollen presentation, which precedes stigma emergence and receptivity. Stigmatic surfaces of both floret types have unicellular, papilloid papillae that are restricted to two ventro-marginal bands on each of the stigmatic arms. Stigmas are characteristic of dry type stigmas and stain positively for polysaccharides, lipids, and an intact cuticle. Cultivars from different origins and with different flowering habits can be synchronized so that flowers of these cultivars release or accept pollen at the same time. Short days have been used by breeders, and genetic gain has been obtained by keeping promising selections under long days in a greenhouse until crossing is performed. Studies on seed development, viability, and the timing of seed maturity are warranted.

LITERATURE CITED

ALEJOS-GONZALEZ, F., G. QU, L.-L. ZHOU, C. H. SARAVITZ, J. L. SHURTLEFF, AND D.-Y. XIE. 2011. Characterization of development and artemisinin biosynthesis in self-pollinated *Artemisia annua* plants. *Planta* 234: 685–697.

ARSENAULT, P. R., D. VAIL, K. K. WOBBE, K. ERICKSON, AND P. J. WEATHERS. 2010. Reproductive development modulates gene expression and metabolite levels with possible feedback inhibition of artemisinin in *Artemisia annua. Plant Physiology* 154: 958–968.

BAILEY, L. H. 1951. Manual of cultivated plants. MacMillan, New York, New York, USA.

BERTIN, R. I., AND C. M. NEWMAN. 1993. Dichogamy in angiosperms. *Botanical Review* 59: 112–152.

BHAKUNI, R., R. JAIN, R. SHARMA, AND S. KUMAR. 2001. Secondary metabolites of *Artemisia annua* and their biological activity. *Current Science* 80: 35–48.

BREMER, K. 1994. Asteraceae: Cladistics and classification. Timber Press, Portland, Oregon, USA.

CRESPO-ORTIZ, M. P., AND M. Q. WEI. 2012. Antitumor activity of artemisinin and its derivatives: From a well-known antimalarial agent to a potential anticancer drug. *Journal of Biomedicine and Biotechnology* 2012: 1–18.

CRUDEN, R. W. 1977. Pollen-ovule ratios: A conservative indicator of breeding systems in flowering plants. *Evolution* 31: 32–46.

DELABAYS, N., X. SIMONNET, AND M. GAUDIN. 2001. The genetics of artemisinin content in *Artemisia annua* L. and the breeding of high yielding cultivars. *Current Medicinal Chemistry* 8: 1795–1801.

DUKE, S. O. AND R. N. PAUL. 1993. Development and fine structure of the glandular trichomes of *Artemisia annua* L. *International Journal of Plant Sciences* 154: 107–118.

FEDER, N., AND T. P. O'BRIEN. 1968. Plant microtechnique: Some principles and new methods. *American Journal of Botany* 55: 123–142.

FERREIRA, J. F. S., AND J. JANICK. 1995. Floral morphology of *Artemisia annua* with special reference to trichomes. *International Journal of Plant Sciences* 156: 807–815.

FERREIRA, J. F. S., J. E. SIMON, AND J. JANICK. 1997. *Artemisia annua*: Botany, horticulture, pharmacology. *Horticultural Reviews* 19: 319–371.

FERRER, M. M., AND S. GOOD-AVILA. 2007. Macrophylogenetic analyses of the gain and loss of self-incompatibility in the Asteraceae. *New Phytologist* 173: 401–414.

GIBSON, J. P., AND A. D. TOMLINSON. 2002. Genetic diversity and mating system comparisons between ray and disk achene seed pools of the heterocarpic species *Heterotheca subaxillaris* (Asteraceae). *International Journal of Plant Sciences* 163: 1025–1034.

GRAHAM, I. A., K. BESSER, S. BLUMER, C. A. BRANIGAN, T. CZECHOWSKI, L. ELIAS, I. GUTERMAN, ET AL. 2010. The genetic map of *Artemisia annua*

L. identifies loci affecting yield of the antimalarial drug artemisinin. *Science* 327: 328–331.

HESLOP-HARRISON, Y. 1977. The pollen–stigma interaction: Pollen tube penetration in *Crocus*. *Annals of Botany* 41: 913–922.

HESLOP-HARRISON, Y., AND K. R. SHIVANNA. 1977. The receptive surface of the angiosperm stigma. *Annals of Botany* 41: 1233–1258.

HISCOCK, S. J., K. HOEDEMAEKERS, W. E. FRIEDMAN, AND H. G. DICKINSON. 2002. The stigma surface and pollen–stigma interactions in *Senecio squalidus* L. (Asteraceae) following cross (compatible) and self (incompatible) pollinations. *International Journal of Plant Sciences* 163: 1–16.

IMBERT, E., J. ESCARRE, AND J. LEPART. 1996. Achene dimorphism and among-population variation in *Crepis sancta* (Asteraceae). *International Journal of Plant Sciences* 157: 309–315.

IMMETHUN, C. M., A. G. HOYNES-O'CONNOR, A. BALASSY, AND T. S. MOON. 2013. Microbial production of isoprenoids enabled by synthetic biology. *Frontiers in Microbiology* 4: 75.

KJAER, A., F. VERSTAPPEN, H. BOUWMEESTER, E. IVARSEN, X. FRETTE, L. P. CHRISTENSEN, K. GREVSEN, AND M. JENSEN. 2013. Artemisinin production and precursor ratio in full grown *Artemisia annua* L. plants subjected to external stress. *Planta* 237: 955–966.

KONOWALIK, K., AND A. KREITSCHITZ. 2012. Morphological and anatomical characteristics of *Artemisia absinthium* var. *absinthium* and its Polish endemic variety *A. absinthium* var. *calcigena*. *Plant Systematics and Evolution* 298: 1325–1336.

LADD, P. G. 1994. Pollen presenters in the flowering plants—Form and function. *Botanical Journal of the Linnean Society* 115: 165–195.

LARSON, T. R., C. BRANIGAN, D. HARVEY, T. PENFIELD, D. BOWLES, AND I. A. GRAHAM. 2013. A survey of artemisinic and dihydroartemisinic acid content in glasshouse and global field-grown populations of the artemisinin-producing plant *Artemisia annua* L. *Industrial Crops and Products* 45: 1–6.

MARTIN, J., M. TORRELL, AND J. VALLES. 2001. Palynological features as a systematic marker in *Artemisia* L. and related genera (Asteraceae, Anthemideae). *Plant Biology* 3: 372–378.

MUCCIARELLI, M., AND M. MAFFEI. 2002. I. Introduction to the genus. *In* C. W. Wright [ed.], *Artemisia*, p. 1-50. CRC Press, Boca Raton, Florida, USA.

OHWI, J. 1965. Graminae.*In* F. G. Meyer and E. H. Walker [eds.], Flora of Japan, 893–898 [English edition]. Smithsonian Institution, Washington, D.C., USA.

OLSSON, M. E., L. M. OLOFSSON, A.-L. LINDAHL, A. LUNDGREN, M. BRODELIUS, AND A. N. D. P. E. BRODELIUS. 2009. Localization of enzymes of artemisinin biosynthesis to the apical cells of glandular secretory trichomes of *Artemisia annua* L. *Phytochemistry* 70: 1123–1128.

PEARCE, A. G. E. 1972. Histochemistry: Theoretical and applied, vol. 2. Churchill Livingstone, London, UK.

PENAS, J., J. LORITE, F. ALBA-SANCHEZ, AND M. A. TAISMA. 2011. Self-incompatibility, flower parameters, and pollen characterization in the narrow endemic and threatened species *Artemisia granatensis* (Asteraceae). *Anales del Jardín Botánico de Madrid* 68: 97–105.

PUGNAIRE, F., AND F. VALLADARES. 2007. Functional plant ecology. CRC Press, Boca Raton, Florida, USA.

TELLEZ, M. R., C. CANEL, A. M. RIMANDO, AND S. O. DUKE. 1999. Differential accumulation of isoprenoids in glanded and glandless *Artemisia annua* L. *Phytochemistry* 52: 1035–1040.

TORRES, C., AND L. GALETTO. 2007. Style morphological diversity of some Asteraceae species from Argentina: Systematic and functional implications. *Journal of Plant Research* 120: 359–364.

WETZSTEIN, H. Y., N. RAVID, E. WILKINS, AND A. P. MARTINELLI. 2011. A morphological and histological characterization of bisexual and male flower types in pomegranate. *Journal of the American Society for Horticultural Science* 136: 83–92.

WIST, T. J., AND A. R. DAVIS. 2008. Floral structure and dynamics of nectar production in *Echinacea pallida* var. *angustifolia* (Asteraceae). *International Journal of Plant Sciences* 169: 708–722.

ZHANG, L., H.-C. YE, AND G.-F. LI. 2006. Effect of developmental stage on the artemisinin content and the sequence characterized amplified region (SCAR) marker of high-artemisinin yielding strains of *Artemisia annua* L. *Journal of Integrative Plant Biology* 48: 1054–1062.